PROCEEDINGS OF SCIENCE

Progress of Jinping Underground Nuclear Astrophysics Experiment (JUNA) project

LIU WeiPing[*a], LI ZhiHong[a], HE JianJun[b], TANG XiaoDong[b], LIAN Gang[a], AN Zhu[c], CHANG JianJun[b], CHEN Han[b], CHEN QingHao[d], CHEN XiongJun[a], CHEN ZhiJun[b], CUI BaoQun[a], DU XianChao[a], FU ChangBo[e], GAN Lin[a], GUO Bing[a], HE GuoZhu[a], HEGER Alexander[f], HOU SuQing[b], HUANG HanXiong[a], HUANG Ning[c], JIA BaoLu[b], JIANG LiYang[a], KUBONO Shigeru[g], LI JianMin[d], LI KuoAng[b], LI Tao[b], LI YunJu[a], LUGARO Maria[h], LUO XiaoBing[c], MA HongYi[b], MA ShaoBo[b], MEI DongMing[i], QIAN YongZhong[j], QIN JiuChang[a], REN Jie[a], SHEN YangPing[a], SU Jun[a], SUN LiangTing[b], TAN WanPeng[k], TANIHATA Isao[l], WANG Shuo[m], WANG Peng[c], WANG YouBao[a], WU Qi[b], XU ShiWei[b], YAN ShengQuan[a], YANG LiTao[d], YANG Yao[b], YU XiangQing[b], YUE Qian[d], ZENG Sheng[a], ZHANG HuanYu[a], ZHANG Hui[d], ZHANG LiYong[b], ZHANG NingTao[b], ZHANG QiWei[a], ZHANG Tao[e], ZHANG XiaoPeng[e], ZHANG XueZhen[b], ZHANG ZiMing[b], ZHAO Wei[d], ZHAO Zuo[a]

[a] *China Institute of Atomic Energy, Beijing, China*
[b] *Institute of Modern Physics, Lanzhou, China*
[c] *Sichuan University, Chengdu, China*
[d] *Tsinghua University, Beijing, China*
[e] *Shanghai Jiaotong University, Shanghai, China*
[f] *Monash University, Melbourne, Victoria, Australia*
[g] *RIKEN, Institute of Physical and Chemical Research, Wako, Japan*
[h] *Konkoly Observatory of the Hungarian Academy of Sciences, Hungary*
[i] *South Dakota State University, Brookings, South Dakota, US*
[j] *Minnesota University, Minneapolis and Saint Paul, Minnesota, US*
[k] *University of Notre Dame, Notre Dame, Indiana, US*
[l] *Osaka University, Suita, Osaka, Japan*
[m] *Shandong University, Weihai campus, Weihai, China*
Email: wpliu@ciae.ac.cn

Jinping Underground laboratory for Nuclear Astrophysics (JUNA) project takes the advantage of the ultra-low background of CJPL lab, high current accelerator and highly sensitive detectors to directly measure a number of crucial reactions occurring at their relevant astrophysical energies. In current phase, JUNA aims at the direct measurements of ^{25}Mg(p,γ)^{26}Al, ^{19}F(p,α)^{16}O, ^{13}C(α,n)^{16}O and ^{12}C(α,γ)^{16}O reactions. The progress, including experimental setup, accelerator system, detector development, and low background test, will be presented.

The 26th International Nuclear Physics Conference
11-16 September, 2016
Adelaide, Australia

*Speaker.

http://pos.sissa.it/

PoS(INPC2016)157

1. Underground laboratory

The ultimate goal of nuclear astrophysics is to understand how nuclear processes generate the energy and synthesize elements in the universe [1]. Great progress in understanding origin of elements and evolution of stars has been made. However, there are still many open questions which need to be solved [2]. Direct measurement of the cross sections for the key nuclear reactions crucial to hydrostatic stellar evolution within Gamow window is one of them. Such data are important for obtaining critical input for stellar model, verifying nuclear physics extrapolation, and constraining theoretical calculations [3].

For the direct measurement of astrophysical reaction rates, one needs to develop high-intensity beams in extremely low background environment, which represents the major challenge at the frontier of nuclear astrophysics. The largest challenge is the extremely small cross section measurement amid large natural and accelerator induced background. The first underground based low-energy accelerator facility, LUNA [4, 5] at Gran Sasso underground laboratory has demonstrated the feasibility of overcoming these challenges. Encouraged by the LUNA experiments, many research programs are proposed in the long-range plan in China, US and Europe.

China JinPing underground Laboratory (CJPL) was established taking advantage of hydropower plants in the Jinping mountain, Sichuan, China [6, 7]. The lab is located near the middle of traffic tunnel. It is shielded by 2400 m of marble rocks. Its ultra-low cosmic-ray background makes it into an ideal environment for low background experiment. CJPL phase I (CJPL-I) is hosting CDEX [8] and PandaX [9] dark matter experiments. CJPL phase II [10] (CJPL-II) has been available at the beginning of 2017 with much larger space (200,000 m^3 volume) than CJPL-I. Jinping Underground laboratory for Nuclear Astrophysics (JUNA) will be the first research program in CJPL-II.

2. Scientific motivation

JUNA aims at direct measurement of (α,γ) and (α,n) reactions in hydrostatic helium burning and (p, γ) and (p, α) reactions in hydrostatic hydrogen burning based on Jinping deep underground laboratory. Currently, many key reaction rates are still with large uncertainties arising from the ambiguity of extrapolation, which are far from the precision requirement by astrophysical models. We plan to measure four key reactions to resolve some of these uncertainties, namely, ^{12}C(α,γ)^{16}O, ^{13}C(α,n)^{16}O, ^{25}Mg(p,γ)^{26}Al and ^{19}F(p,α)^{16}O. In the following sections, the experimental plan and progress of detector development are given respectively.

2.1 ^{12}C(α,γ)^{16}O

The ^{12}C(α,γ)^{16}O reaction is often quoted as the holy grail in nuclear astrophysics [1]. The uncertainty of this reaction affects not only the nucleosynthesis of elements up to iron, but also the evolution of the massive stars and their final fates. The cross section of this reaction is desired to be known within less than 10% at helium burning temperatures (T_9=0.2), corresponding to a Gamow window around $E_{c.m.}$=300 keV. It is extremely difficult to directly measure the reaction cross section (about 10^{-17} barn) at this energy [11]. Current ground based technology can only achieve 10^{-14} barn cross section level in $E_{c.m.}$=900 keV.

A direct measurement at $E_{c.m.}$=600 keV will be done in JUNA with high intensity $^4He^{2+}$ beam as the first step to provide a better constrain for extrapolating models [12]. We will measure the angular distribution with High-Purity Germanium detectors (HPGe) firstly,and ultimately measure the total cross section at $E_{c.m.}$=600 keV with a BGO detection array with an expected precision of 10%. As a try, the test measurement at $E_{c.m.}$=380 keV with BGO array will be done. Fig. 1 shows the setup of four HPGe detectors and the high-purity ^{12}C target.

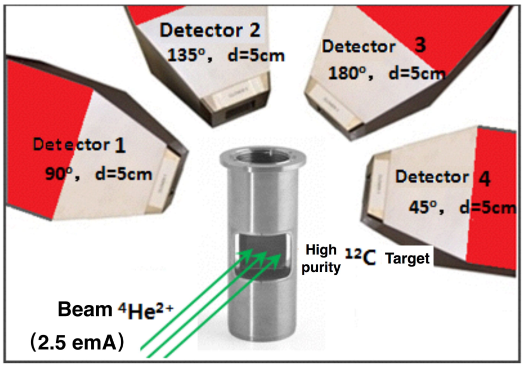

Figure 1: Schematic of $^{12}C(\alpha,\gamma)^{16}O$ detection setup.

For total cross section measurement at $E_{c.m.}$=600 keV, based on the experimental angular distribution, we will optimize the experimental conditions, 1) optimizing the beam transmission and the shielding to suppress the background induced by the beam, 2) confirming the origin of ^{13}C and improving the implantating condition of ^{12}C implanted target to minimize ^{13}C impurity. The BGO detection array placed around the target chamber can significantly increase the detection efficiency (absolute efficiency 75% at E_γ = 6 MeV) of γ-rays. With the improvement above, an accurate total cross section will be obtained.

For test measurement at $E_{c.m.}$=380 keV, we will use $^4He^{2+}$ beam at an intensity of 2.5 emA and an energy of 507 keV ($E_{c.m.}$=380 keV) togethor with the high-efficiency BGO detection array. Thus, the total cross section of $^{12}C(\alpha,\gamma)^{126}O$ in the energy region of near Gamow window can be challenged.

2.2 $^{13}C(\alpha,n)^{16}O$ reaction

The $^{13}C(\alpha,n)^{16}O$ reaction is the key neutron source reaction for the stellar s-process nucleosynthesis. Due to the existence of sub-threshold resonances, there is a rather large uncertainty (~30%) in this important reaction rate which limits our understanding to the nucleosynthesis of heavy elements. We will take the advantage of the ultra low background in Jinping underground lab, the first underground high current accelerator based on an ECR source and high sensitive neutron detector to study directly this important reaction for the first time at energies down to $E_{c.m.}$ ~0.2 MeV, within its relevant stellar energy range [13].

We are designing a fast neutron detector consisting of 24 ^{3}He proportional counters and a liquid scintillator. The schematic setup of the detector is shown in Fig. 2. The scintillator has a cylindrical shape with a length of 0.4 m and a diameter of 0.4 m. The 24 ^{3}He counters are distributed in the two circles with radii of 0.1 m and 0.15 m, respectively.

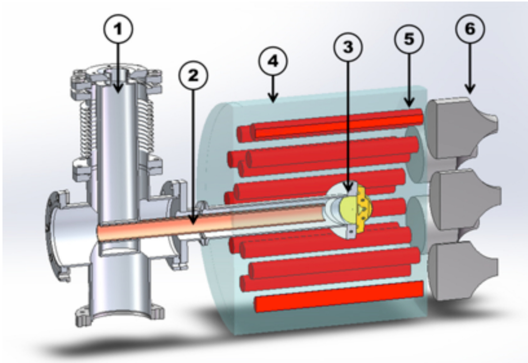

Figure 2: Schematic drawing of low background highly sensitive fast neutron detector. 1) LN_2 cold trap; 2) Copper tube; 3) high power ^{13}C target; 4) Liquid scintillator; 5) ^3He detectors; 6) PMTs.

The energies of neutrons from the $^{13}C(\alpha,n)^{16}O$ reaction are in the range of 2 to 3 MeV. The produced neutrons are firstly slowed down by the liquid scintillator. After their thermalization, some neutrons enter ^3He counters and are detected. With the coincidence between the fast signal from fast neutron slowing down inside the liquid scintillator and the delayed signal from the thermalized neutrons captured by the ^3He counters, we can effectively suppress the backgrounds in liquid scintillator and ^3He detectors. The detection efficiency after coincidence is estimated to be 20% for neutrons from the $^{13}C(\alpha,n)^{16}O$ reaction.

However, the coincidence cannot easily remove the correlated background. For example, in the decay chain of U/Th impurities in the stainless steel walls of ^3He counters, there is a possibility that some product emits β particle and then α decay. If the α particle enters the liquid scintillator while the β triggers the liquid scintillator, a correlated event will be recorded. To suppress this kind of background, we plan to analyze the waveforms from ^3He counters to select the neutron events and reject α events. As a tradeoff, the efficiency of the ^3He counters will be decreased by a factor of 2. Therefore, the detection efficiency with coincidence between the ^3He counters and the liquid scintillator drops to 10%.

2.3 ^{25}Mg(p,γ)^{26}Al

The $^{25}Mg(p,\gamma)^{26}Al$ reaction is believed to be the main path to produce ^{26}Al in the galaxy and its cross section are dominated by the capture process of the isolated resonances in ^{26}Al. The temperature range of astrophysical interests is T = 0.02-2 GK, so the resonances between 50 and 310 keV are more important in this study. Many experiments have been performed to study the $^{25}Mg(p,\gamma)^{26}Al$ reaction sine 1970 [14, 15, 16, 17, 18, 19, 20, 21, 22, 23, 24, 25], but the experiment on the surface of the earth can only reach to energies above $E_{c.m.}$=190 keV due to the small cross section and large background induced by the cosmic rays. In 2012, the resonance strength at 92 keV was successfully measured under the ultra-low background condition in the Laboratory of Underground Nuclear Astrophysics (LUNA) in Italy [26, 27]. However, resonance at $E_{c.m.}$=58 keV is still inaccessible for direct measurement in the shielding conditions of LUNA experiments. Benefiting from the ultra low background at CJPL and the high beam intensity, we will be able to measure the resonance strength at $E_{c.m.}$=58 keV with a 4π BGO γ detectors array, as shown in Fig 3.

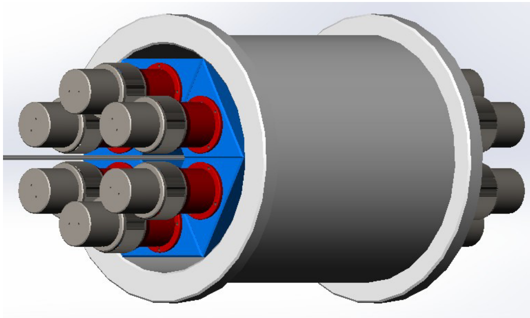

Figure 3: The 4π BGO γ-ray detector designed for JUNA.

Table 1: Basic parameters of four reactions planned.

Reaction	Beam type	Beam (emA)	$E_{c.m.}$ (keV)	σ or $\omega\,\gamma$	Target	Eff %	Event (/day)	BG (/day)
^{12}C(α,γ)^{16}O	^{4}He^{2+}	2.5	380	10^{-13} mb	10^{18} cm^{-2}	75	0.7	0.7
^{13}C(α,n)^{16}O	^{4}He^{1+}	10	200	4×10^{-11} mb	Thick	20	7	1
^{25}Mg(p,γ)^{26}Al	^{1}H^{1+}	10	58	2.1×10^{-13} eV	0.6 μg/cm^2	38	1.4	0.7
^{19}F(p,α_γ)^{16}O	^{1}H^{1+}	0.1	100	7.2×10^{-9} mb	4 μg/cm^2	75	27	0.7

In order to optimize the experimental setup for the ^{25}Mg$(p,\gamma)^{26}$Al reaction at JUNA, the resonance strength at $E_{c.m.}$=58 keV has been estimated whih a shell model calculation. The results show that the ^{25}Mg$(p,\gamma)^{26}$Al reaction rate at $T < 0.06$ GK is dominated by this resonance at $E_{c.m.}$=58 keV [28]. The thick-target yield of the 58 keV resonance is estimated under the conditions of JUNA with 10 mA proton beams and 4π BGO γ-ray detector. The maximum yield is proportional to the resonance strength by

$$Y_{max}(\infty) = \frac{\lambda_r^2}{2}\omega\gamma\frac{M+m}{M\varepsilon_r}, \tag{2.1}$$

where λ_r and ε_r are the de Broglie wavelength and stopping power at resonant energy, M and m are the mass of the target and projectile nuclei, respectively. According to the calculation with Eq. (2.1), the counting rate of the ^{25}Mg$(p,\gamma)^{26}$Al reaction at $E_{\rm c.m.}$ = 58 keV is about 1.4 events per day. The background counting rate is estimated to be less than 0.2 events per day. Thus we can accumulate around 40 real events in one month, and the statistical uncertainty will be about 16%.

2.4 ^{19}F(p,α)^{16}O

The ^{19}F(p,α)^{16}O reaction is considered to be an important reaction in the CNO cycles. Currently, the experimental cross sections of this reaction at Gamow energies are still incomplete, and the precision of its thermonuclear reaction rate does not yet satisfy the model requirement. The proposed experiment is targeting on direct cross section measurement of the key ^{19}F(p,α)^{16}O reaction right down to the Gamow energies (70–350 keV in the center-of-mass frame) with a precision better than 10 % [29].

Table 2: Comparison of the goal for four reaction with current status.

reaction	physics	current (keV)	current uncertainty(%)	ref.	JUNA (keV)	expected uncertainty (%)
^{12}C(α,γ)^{16}O	Massive star	890	60	[30]	380	test
^{13}C(α,n)^{16}O	s-process neutron source	279	60	[31]	200	20
^{25}Mg(p,γ)^{26}Al	Galaxy ^{26}Al source	92	20	[26]	58	15
^{19}F(p,α_γ)^{16}O	Fluorine overabundance	189	80	[32]	100	10

A 'lamp'-type Micron silicon array will be constructed for the charged particle measurement, which can cover about 4π solid angle. This universal detection array will set the base for studying the charged-particle-induced reactions at JUNA. A conceptual design is shown in Fig. 4. It can not only measure the total (p,α_0) cross section but also the angular distribution. The experimental angular distribution is very useful for revealing nuclear structure of the low-energy resonances. In this experiment, a thin target of about 4 μg/cm^2 CaF_2 will be utilized, which is evaporated on a thin metal backings. Thanks to the high Q value (about 8.11 MeV) for this reaction, the average energy for the emitted α particles is about 6.7 MeV. These relatively high-energy particles can penetrate the backings and be detected easily at the forward angle. The detectors at the forward angle do not face the Rutherford-scattered strong proton beam which is stopped in the backings. However, those detectors at the backward angle should be shielded by a thin foil, e.g., a mylar foil, to stop the scattered protons. The target backing will be connected to a cooling device to release the heat during the experiment.

As for the ^{19}F(p,α_γ)^{16}O channel, the energies of emitted γ rays are about 6–7 MeV. In this project, two γ detection arrays are now been constructed: one is a HPGe array whose absolute detection efficiency is about 1% for the γ rays of interest with excellent energy resolution; another one is the 4π BGO array as introduced above, whose absolute efficiency is about 75%, but with moderate resolution. Here, the HPGe array will be utilized in the $E_{c.m.}$>140 keV energy region (with higher cross sections), while the BGO array will be used below this energy region (with lower cross sections). With the excellent resolution of the HPGe detector, the possible contaminations can be resolved and identified clearly, which makes the BGO γ-ray identification reliable at lower-energy region. A conceptual design for the HPGe array is shown in Fig. 5.

2.5 Summary of event and background

The event rate of the four reactions are estimated according to the current best data. The background rate are deduced from the measured data of rock, detector in CJPL-I environment, plus the estimated one induced by accelarator. The rates are summarized in Tab. 1. We also compared our expected precision with current experimental results. The results are summarized in Tab. 2.

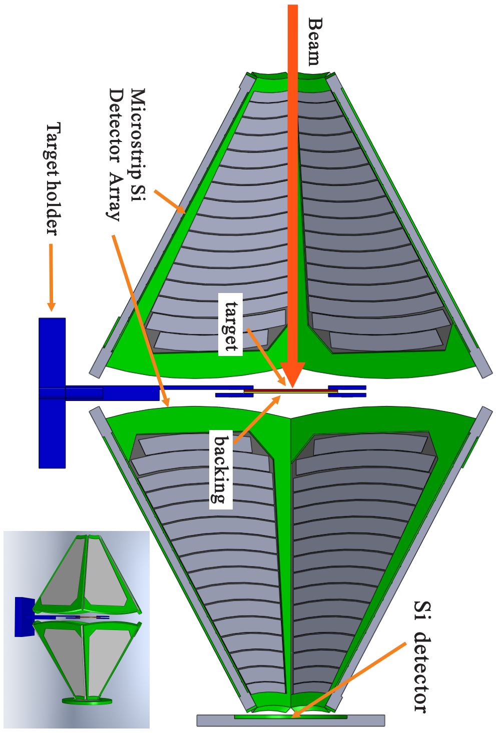

Figure 4: Conceptual silicon detector array designed for measuring the charged particles.

3. Accelerator, detector and shielding system

The key techniques, which include the accelerator system with high stability and high intensity, the detector detection system, and the shielding material with ultra-low background, will be developed through the above research.

The preliminary design of the low energy and high current accelerator system of JUNA is shown in Fig. 6. For ensuring the four reaction measurement, we plan to optimize the accelerator system based on the following consideration [33].

3.1 2.45 GHz ECR ion source and Low Energy Beam Trasport Line

We adopted a design of 2.45 GHz ECR which was developed for the CI-ADS project. This ion source is expected to delivered 12 emA proton, 6 emA He^{+} and 2.5 emA He^{2+}. The maximum beam energy out of ion source is 50 keV/q with emittance less than 0.2 π·mm·mrad. The Low Energy Beam Transport line (LEBT) is designed to minimize the space charge effect and improve the beam transport efficiency. Beam will be accelerated before being focused with two solenoids. To keep the LEBT as short as possible, all the steering magnets are built inside of the solenoids. He^{2+} beam is expected to be mixed with a large fraction of He^{+} beam. A 30 deg magnet will be added between the two solenoids to filter out the intense He^{+} and reduce the burden of the acceleration tube.

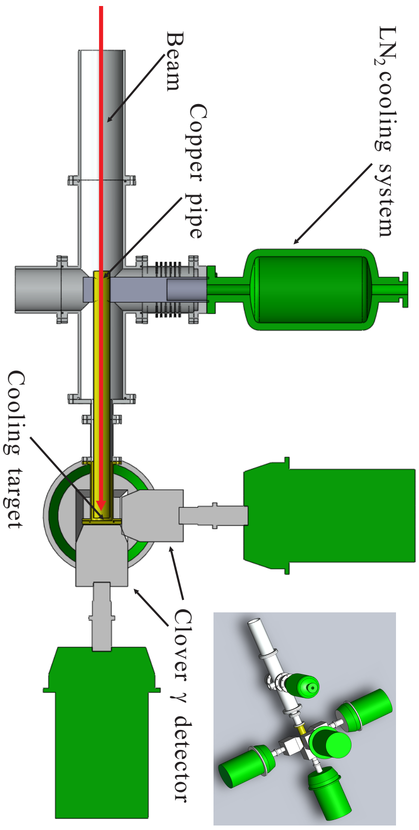

Figure 5: Conceptual HPGe detector array designed for measuring the γ rays.

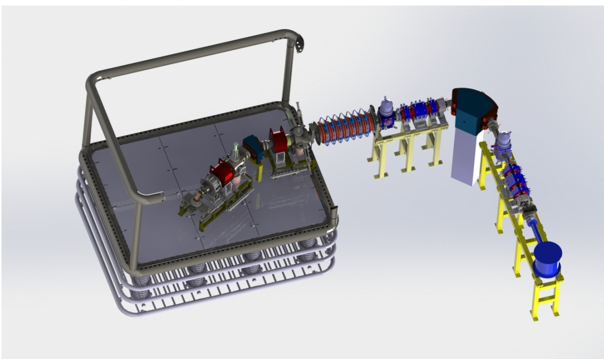

Figure 6: Design of the low energy and high current accelerator system.

3.2 Developing a high stability power supply system

For JUNA project, the long-term stability is one of the critical parameters to ensure the high measurement precision. Hence the high-voltage power supply with high stability must be used. We plan to cooperate with Glassman High Voltage, Inc and develop a 400 kV, 6 kW high stability power supply (long-term output voltage stability 0.05%, ripple voltage 0.01%).

3.3 Optimizing the design of the accelerating tube

As for the low energy and high intensity beam, the space-charge effect must be controlled during transmission in order to increase the transport efficiency. The high transport efficiency could not only ensure enough beam intensity on target, but also reduce the background brought by the beam itself. We plan to adopt segmental voltage supply for the accelerating tube and design an acceleration and deceleration structure for the accelerating tube electrode to reduce the space-charge effect.

3.4 The design of the experimental space and shielding system

The effect to background ratio of the nuclear reaction measurement will be significantly enhanced with the ultra-low background of CJPL and high current beam. But at the same time the high current beam will bring beam induced background, which must be effectively shielded. We plan to construct two shielding systems around the target chamber and the detectors, aiming at shielding γ-ray and neutron, respectively.

In order to avoid the influence to other laboratories in CJPL, we plan to cover the accelerating tube with Lead shielding layer and build a concrete shielding wall in our laboratory to block the background coming from accelerator.

For experimental space, we will use A1 space of CJPL-II. Currently, the physical floor plan is fixed, and now is under engineering design. The decoration of the space is scheduled in the second quarter of 2016 and will be ready for accelerator on site tuning by the end of June 2016.

3.5 The development of the high power solid target

In order to keep the stability of the solid target under the bombardment of mA intensity beam, we are developing a high power solid target system. The temperature of target will be effectively controlled by rotational design of heat conduction and water cooling. The expected power of the solid target system will be 20 kW/cm^2, which will satisfy the requirement of the above experiments.

4. Summary and conclusion

JUNA experiment is in progress in all aspects. The accelerator system and detector array will be installed and commissioned by the end of 2017, four experiments will be performed one by one from 2018 and the first batch of experimental results will be delivered by the end of 2019.

In summary, a new underground nuclear astrophysics experiment JUNA is being developed at Jinping, China. JUNA will study the four key nuclear reactions of star evolution. Taking the advantage of great environments of CJPL-II, high intensity accelerator, and high efficiency detectors, JUNA will be able to take a favorable position among underground nuclear astrophysics laboratories in the world.

PoS(INPC2016)157

References

[1] Rolfs C and Rodney W S, Cauldrons in the Cosmos, The University Chicago Press, 1988

[2] Haseltine E, The 11 Greatest Unanswered Questions of Physics, Discover Magazine, 2002, 23: 2

[3] Iliadis C, Nuclear Physics of Stars, Wiley-VCH Verlag GmbH, 2007

[4] Formicola A, Imbriani G, Junker M, et al. The LUNA II 400 kV accelerator[J]. Nuclear Instruments & Methods in Physics Research, 2003, 507(3):609-616.

[5] Costantini H, Formicola A, Imbriani G, et al. LUNA: a Laboratory for Underground Nuclear Astrophysics[J]. Reports on Progress in Physics, 2009, 972(8):086301.

[6] Chen H S, Deep underground physics[J], Science(in Chinese), 2010, 62: 4

[7] Cheng J P, Wu S Y, Yue Q, et al. Development of underground laboratory in the world[J]. Physics (in Chinese), 2011, 03(03):149-154.

[8] Zhao W, Yue Q, Kang K J, et al. First results on low-mass WIMP from the CDEX-1 experiment at the China Jinping underground Laboratory[J]. Physical Review D, 2013, 88(5):1201-1205.

[9] Cao X G, Chen X, Chen Y H, et al. PandaX: a liquid xenon dark matter experiment at CJPL. Sci China-Phys Mech Astron, 2014, 57(8): 1476-1494.

[10] Normile D. Physics. China supersizes its underground physics lab.[J]. Science, 2014, 346(6213):1041-1041.

[11] Buchmann L, Nuclear Physics A, 2005, 758:355c-362c.

[12] Liu W P, The ^{12}C(α,γ)^{16}O reaction proporsal, 2014, unpublished.

[13] Tang X D, The ^{13}C(α,n)^{16}O reaction proporsal, 2014, unpublished.

[14] Betts R R, Fortune H T, Pullen D J. A study of ^{26}Al by the ^{25}Mg(^{3}He, d) reaction[J]. Nuclear Physics A, 1978, 299(3):412-428.

[15] Champagne A E, Howard A J, Parker P D. Threshold states in ^{26}Al: (I). Experimental investigations[J]. Nuclear Physics A, 1983, 402(1):159178.

[16] Champagne A E, Howard A J, Parker P D. Threshold states in ^{26}Al: (II). Extraction of resonance strengths[J]. Nuclear Physics A, 1983, 402(1):179188.

[17] Endt P M, de Wit P, Alderliesten C. The ^{25}Mg(p, γ) ^{26}Al and ^{25}Mg(p, p') resonances for E_p = 0.31-1.84 MeV[J]. Nuclear Physics A, 1986, 459(1):61-76.

[18] Champagne A E, Nald A B, Wang T F, et al. Threshold states in ^{26}Al revisited[J]. Nuclear Physics A, 1986, 451(3):498-508.

[19] Endt P M, Rolfs C. Astrophysical aspects of the ^{25}Mg(p, γ)^{26}Al reaction[J]. Nuclear Physics A, 1987, 467(2):261272.

[20] Champagne A E, Howard A J, Smith M S, et al. The effect of weak resonances on the ^{25}Mg(p, γ)^{26}Al reaction rate[J]. Nuclear Physics A, 1989, 505(2):384396.

[21] Rollefson A A, Wijekumar V, Browne C P, et al. Spectroscopic factors for proton unbound levels in ^{26}Al and their influence on stellar reaction rates[J]. Nuclear Physics A, 1990, 507(2):413425.

[22] Iliadis C, Schange T, Rolfs C, et al. Low-energy resonances in ^{25}Mg(p, γ)^{26}Al, ^{26}Mg(p, γ)^{27}Al and ^{27}Al(p, γ)^{28}Si[J]. Nuclear Physics A, 1990, 512(3):509530.

[23] Iliadis C, Buchmann L, Endt P M, et al. New stellar reaction rates for ^{25}Mg(p, γ)^{26}Al and ^{25}Al(p, γ)^{26}Si[J]. Physical Review C, 1996, 53(1):475-496.

[24] Powell D C, Iliadis C, Champagne A E, et al. Low-energy resonance strengths for proton capture on Mg and Al nuclei[J]. Nuclear Physics A, 1998, 644(4):263276.

[25] Arazi A, Faestermann T, Niello J O F, et al. Measurement of ^{25}Mg(p, γ)^{26}Al^{g} resonance strengths via accelerator mass spectrometry[J]. Physical Review C, 2006, 74(2):025802.

[26] Strieder F, Limata B, Formicola A, et al. The ^{25}Mg(p, γ)^{26}Al reaction at low astrophysical energies[J]. Physics Letters B, 2012, 707:6065.

[27] Straniero O, Imbriani G, Strieder F, et al. Impact of a Revised ^{25}Mg(p, γ)^{26}Al Reaction Rate on the Operation of the Mg-Al Cycle[J]. Astrophysical Journal, 2013, 763(2).

[28] Li Z H, Su J, Li Y J, et al. Determination of the ^{25}Mg(p, γ)^{26}Al resonance strength at $E_{c.m.}$=58 keV via shell model calculation[J], Science China Physics, Mechanics & Astronomy, 2015, 58.

[29] He J J, Xu S W, Ma S B, et al. A proposed direct measurement of cross section at Gamow window for key reaction ^{19}F(p, α)^{16}O in Asymptotic Giant Branch stars with a planned accelerator in CJPL[J]. Science China Physics, Mechanics & Astronomy, 2016, 59(5): 1-7.

[30] Hammer J W, Fey M, Kunz R, et al. E1 and E2 capture cross section and astrophysical reaction rate of the key reaction ^{12}C(α, γ)^{16}O[J]. Nuclear Physics A, 2005, 758:363366.

[31] Drotleff H W, Denker A, Knee H, et al. Reaction rates of the s-process neutron sources ^{22}Ne(α, n)^{25}Mg and ^{13}C(α, n)^{16}O[J]. Astrophysical Journal, 1993, 414:735-739.

[32] Lombardo I, Dell'Aquila D, Leva A D, et al. Toward a reassessment of the ^{19}F(p,α_0)^{16}O reaction rate at astrophysical temperatures[J]. Physics Letters B, 2015:178182.

[33] Lian G, The JUNA platform proporsal, 2014, unpublished.

PoS(INPC2016)157